Metallic transmission screen for sub-wavelength focusing

A.M.H. Wong, C.D. Sarris and G.V. Eleftheriades

A simple metallic transmission screen is proposed that is capable of focusing an incident plane wave into a sub-wavelength spot in the near field. The principle of operation is inspired by holographic concepts applied to the near-field. A corresponding design procedure is described and supporting full-wave simulation results are provided.

Introduction: Strong recent interest has centred on near-field imaging systems which produce sub-wavelength resolution. These imaging systems promise increased capabilities in microscopy, lithography, and near-field sensing as well as other applications [1–3]. This Letter describes a simple yet novel metallic transmission screen which focuses an incident electromagnetic wave to a sub-wavelength spot in the near field. The transmission screen was inspired by concepts from holography, where a record of the interference between two waves is used to convert a reference waveform into the desired object waveform [4]. In the remaining sections of this Letter, we explain our two-stage design process, in which we first design an appropriate (in general complex) transmission function, and then implement it with a binary metallic screen. We also display corresponding results from a scalar diffraction calculation and a full-wave simulation demonstrating sub-wavelength resolution.
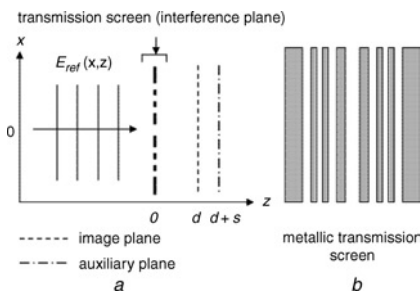

Fig. 1 *Diagram depicting setup of transmission screen; metallic transmission screen designed for focusing 3 GHz incident plane wave to sub-wavelength spot at image plane*

a Setup of transmission screen
b Metallic transmission screen for focusing 3 GHz incident plane wave to sub-wavelength spot at image plane
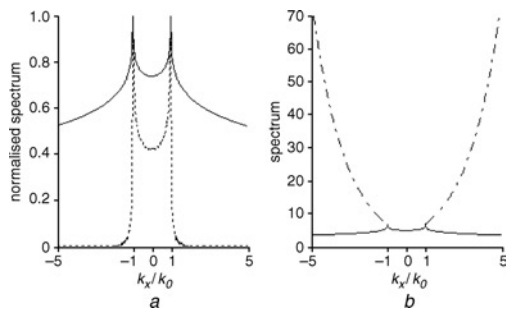

Fig. 2 *Comparing normalised spectrum at auxiliary plane $s = 0.001\lambda$ (solid) and plane 0.5λ to right of image plane (dot) shows that $E_{con}(x, y) = \exp(ikr)/r$ contains significant evanescent components in near field (Fig. 2a); comparison of spectra at auxiliary plane (solid) and interference plane (dash-dot) (Fig. 2b)*

Design of transmission function: Fig. 1 shows a diagram depicting our problem of transmission function design. We use, as the reference wave, a normally incident plane wave described by $E_{ref}(x, z) = \exp(-ik_0 z)$, and desire to reconstruct a converging wave described by

$$E_{con}(x, z) = \exp(ikr)/r \quad \text{where} \quad r = \sqrt{x^2 + (z - d)^2} \qquad (1)$$

where d represents the focal distance. In operation, the transmission function will be multiplied with the reference waveform to form a new waveform E_{rec} immediately to the right of the interference plane, which will reconstruct E_{con} at the image plane. While the choice of

the field distribution at the image plane is in general arbitrary, we have been motivated to reconstruct E_{con} in the form of (1) because earlier work on a negative-refractive-index slab lens [5] has revealed similar field variation close to and to the right of the image plane (i.e. away from the lens). Furthermore, the near-field spectrum of (1) has ample evanescent-wave components (see Fig. 2), thus allowing image formation with sub-wavelength resolution (other suitable evanescent-wave 'rich' distributions would include $\exp(jkr)/r^2$, etc.).
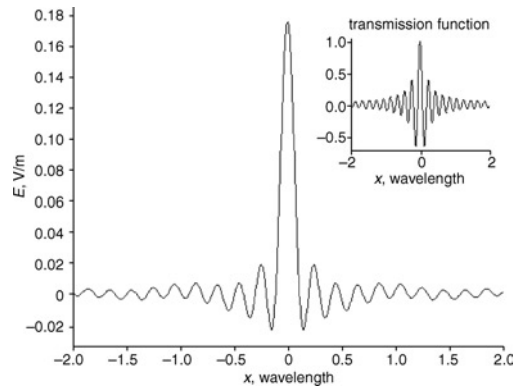

Fig. 3 *Field distribution at image plane, after applying transmission function to reference wave E_{ref}, with field amplitude 1 V/m*

Real part of field, which comprises more than 98% of electric field energy, is shown in Figure. Focal width at half maximum is 0.13λ
Inset: design transmission function

We now outline an approach to designing a general transmission function $T(x)$, which converts an arbitrary electric field E_{ref} into a chosen E_{con} at the image plane. Although we have, for simplicity, chosen to assume 2D propagation (i.e. $\partial/\partial y = 0$ in Fig. 1), the following procedure can be naturally extended to a 3D scenario. We seek to determine, through the principle of back-propagation, the desired waveform E_{rec} at the interference plane which will lead to the waveform E_{con} at the image plane. First, we expand our desired converging wave (1) as a spectrum of propagating and evanescent plane waves along an auxiliary plane, a short distance s to the right of the image plane (see Fig. 1):

$$S(k, z = d + s) = \int_{-\infty}^{+\infty} E_{con}(x, z = d + s) \exp(-ik_x x) dx$$

$$= k_0 \left(is \sqrt{k_0^2 - k_x^2} \right) \qquad (2)$$

where k_o is the zero order modified Bessel function of the second kind. Note that the image plane ($z = d$) was avoided due to the singularity caused by the implied presence of a source by (1), which cannot be physically reproduced by the superposition of plane waves. Moreover, all evanescent waves decay in the $+z$ direction, hence evanescent components are enhanced as they are back-propagated from the auxiliary plane to the interference plane; this enhancement of evanescent components is crucial to obtaining sub-wavelength focusing capability. We may now express the spectrum at the interference plane as

$$S(k_x, z = 0) = K_0(isk_z) \exp(-ik_z(s + d)),$$
$$\text{where } k_z = \sqrt{k_0^2 - k_x^2} \qquad (3)$$

Finally, we perform an inverse Fourier transform to obtain E_{rec}. After obtaining E_{rec}, we can easily find the required transmission function of the screen by $T(x) = E_{rec}(x)/E_{ref}(x, z = 0) = E_{rec}(x)$. ($E_{ref} = 1$ for a normally incident plane wave.) We follow the above procedure to design a transmission function which converts a normally incident plane wave into a waveform focusing at a distance of $d = \lambda/10$. To handle the diverging nature of the spectrum (3) we have truncated it to a bandwidth of $[-5k_0, 5k_0]$. This implies that the actual spectrum to be reconstructed (2) is truncated to a maximum wavenumber $|k_{xm}| = 5k_o$. Since this bandwidth is five times the bandwidth of conventional imaging systems, which transmit only propagating waves, we expect the optimal focusing quality of the resulting screen to be about $\lambda/10$, a fivefold improvement over the diffraction limit. Fig. 2 shows the spectra at the auxiliary plane (solid) and the interference

plane (dash-dot). A growth in the evanescent components can be clearly observed at the interference plane. The inset of Fig. 3 shows the real part of the designed transmission function. This function has a (sub-wavelength) periodicity which matches that of the bandwidth limit (k_{xm}); this is essential for encoding the sub-wavelength information onto the screen. Fig. 3 shows the corresponding field distribution along the image plane of which the full width at half maximum (FWHM) is 0.13λ. This is indeed roughly a fivefold improvement over the FWHM of 0.6λ for a diffraction-limited sinc(x) function. We note that higher resolution can be obtained by simply using a wider bandwidth $|k_{xm}|$, thus resulting in a correspondingly narrower focal width. However, this is associated with an attenuation in magnitude from the screen to the image plane of the order of $\exp(-k_{xm}d)$.

Table 1: Locations and sizes of slits on metallic screen (see Fig. 1)

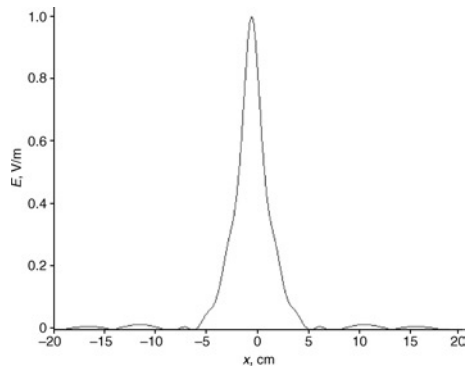| Centre	Width
$0\lambda/0$ mm	$0.144\lambda/14.4$ mm
$\pm 0.241\lambda/\pm 24.1$ mm	$0.062\lambda/6.2$ mm
$\pm 0.450\lambda/\pm 45.0$ mm	$0.062\lambda/6.2$ mm
$\pm 0.658\lambda/\pm 65.8$ mm	$0.075\lambda/7.5$ mm

Fig. 4 *Full-wave field distribution at image plane (normalised), after shining normally incident 3 GHz plane wave E_{ref} onto designed metallic screen*

Focal width at half maximum is 0.25λ, as opposed to diffraction limited pattern of 0.6λ. For this simulation, screen was embedded in larger ground plane to avoid edge diffracted effects

Metallic screen implementation of transmission function: Using a metallic screen, we have implemented a close approximation to our transmission function, following a technique inspired by earlier work on far-field microwave holographic antennas [6]. In holography, the transmission function is the intensity of the interference pattern of the object and reference waveforms:

$$T_{approx}(x) = \|E_{ref}(x, z=0) + E_{rec}(x)\|^2$$
$$= 1 + 2\,\mathrm{Re}\{E_{rec}(x)\} + \|E_{rec}(x)\|^2 \qquad (4)$$

Upon reconstruction, one retrieves the image E_{rec}, and the conjugate image E_{rec}^* and two other terms contributing to zero-order transmission. Since these zero-order transmission terms only contribute to background noise, we suppress them to obtain $T'_{approx}(x) = \mathrm{Re}\{E_{rec}(x)\}$. To realise this function with metallic strips and slits, we follow [6] in placing metal strips to represent the transmission function's periodicity and fringe width. However, while [6] padded positive (high intensity) fringes with metallic strips, we pad the negative cycles of $T'_{approx}(x)$ with metallic strips. We also slightly alter the sizes of metallic strips

such that the field amplitudes transmitted by the sidelobes are in proportional agreement with those described in $T'_{approx}(x)$. Fig. 1 shows a diagram of the transmission screen, and Table 1 summarises the locations and widths of the slits on the metallic screen. Full-wave simulations with COMSOL at 3 GHz show a FWHM of 0.25λ at a distance 0.1λ away from the metallic screen. The corresponding magnitude of the electric field at this image plane is shown in Fig. 4. As shown, the focusing quality of the metallic screen does not fully match that of the complex screen. It can be shown that this mismatch can be mainly attributed to the inability of a binary screen to produce both positive and negative field values (see inset of Fig. 3). This produces a non-zero 'DC' distribution around $k_x = 0$ which superimposes on the desired distribution at the image plane of Fig. 3 and produces the observed beam widening in Fig. 4 near the null-points. Nevertheless, the obtained FWHM of 0.25λ still represents a dramatic improvement over the diffraction-limited FWHM of 0.6λ.

Conclusions: Through holographic principles applied to the near-field, we have prescribed a method for implementing simple metallic transmission screens, capable of focusing incident electromagnetic waves into sub-wavelength spots in the near field. It should be noted that while preparing this manuscript, a recent paper [7] came to our attention describing related near-field focusing structures. However the formulation in [7] is quite different and is not based on the principle of holography; in fact [7] only accounts for the focusing of evanescent waves. Moreover, [7] merely proposes specific screen current distributions but not any specific physical structures that produce these required currents. Finally, the structures of [7] require positive and negative index regions. In contrast, we propose readily realisable holographic screen patterns that only require simple slits cut on a ground plane.

A.M.H. Wong, C.D. Sarris and G.V. Eleftheriades (*Department of Electrical and Computer Engineering, University of Toronto, 10 King's College Road, Toronto, ON M5S 3G4, Canada*)

E-mail: gelefth@waves.utoronto.ca.

References

1 Pendry, J.B.: 'Negative refraction makes a perfect lens', *Phys. Rev. Lett.*, 2000, **85**, (18), pp. 3966–3969
2 Salandrino, A., and Engheta, N.: 'Far-field subdiffraction optical microscopy using metamaterial crystals: theory and simulatiaons', *Phys. Rev. B*, 2006, **74**, p. 075103
3 Freire, M.J., and Marqués, R.: 'Planar magnetoinductive lens for three-dimensional subwavelength imaging', *Appl. Phys. Lett.*, 2005, **86**, p. 182505
4 Goodman, J.W.: 'Introduction to Fourier optics' (Roberts & Company, Englewood, CO, 2005)
5 Grbic, A., and Eleftheriades, G.V.: 'Negative refraction, growing evanescent waves, and subdiffraction imaging in loaded transmission-line metamaterials', *IEEE Trans. Microw. Theory Tech.*, 2003, **51**, (12), pp. 2297–2305
6 Checcacci, P.F., Russo, V., and Scheggi, A.M.: 'Holographic antennas', *IEEE Trans. Antennas Propag.*, 1970, pp. 811–813
7 Merlin, R.: 'Radiationless electromagnetic interference: evanescent-field lenses and perfect focusing', *Science*, 2007 (10.1126/science.1143884)